

## Models for Comparative Analysis, Assessment and Adoption of Preferred Experimental Techniques

Chukwuka Ikechukwu Nwoye\*<sup>1</sup>, Chizoba Chinedu Nwoye<sup>2</sup>, Martin Obi<sup>3</sup>, Gideon Obasi<sup>4</sup> and Okechukwu Onyebuchi Onyemaobi<sup>1</sup>

<sup>1</sup> Department of Materials and Metallurgical Engineering, Federal University of Technology, Owerri, Nigeria.

<sup>2</sup> Data Processing, Modelling and Simulation Unit, Weatherford Nig. Ltd. Port-Harcourt Nigeria.

<sup>3</sup> Department of Industrial Mathematics, Federal University of Technology, Owerri, Nigeria.

<sup>4</sup> Department of Material Science, Aveiro University, Portugal

[chikeyn@yahoo.com](mailto:chikeyn@yahoo.com)

**Abstract:** Models for comparative analysis, assessment and adoption of preferred experimental techniques have been derived. The models were used to analyze and assess data culled from the varying electrical properties associated with the various techniques applied for the casting of Pb-Sb-Cu alloys (designated for use in the manufacturing of battery head terminals and plates) with the view to adopting the ideal and preferred experimental technique. Technique A, involved simultaneous addition of Cu powder and pouring of the molten Pb-Sb into the mould, Technique B involved addition of Cu powder intermittently as pouring of Pb-Sb into the mould was going on while Technique C involved pouring a stirred mixture of heated Pb-Sb alloy and powdered Cu into the mould. The results of the analysis carried out using these models agree completely with past experimental report that Technique A (having permitted greater amount of current flow through the associated alloys) is the most ideal and preferred technique (amongst the other three techniques) for casting Pb-Sb-Cu alloys expected to have enhanced electrical properties. [New York Science Journal. 2010;3(1):42-49]. (ISSN: 1554-0200).

**Keywords:** Model, Analysis, Assessment, Adoption, Preferred Experimental Techniques.

### 1. Introduction

Models are tools for the theoretical and experimental analysis of processes. It has been reported (Iwu,1996) that model can be used for estimation, prediction, optimization and calibration of process data. The values of output process-parameters in most engineering processes could be estimated predicted or optimized providing the values of the input parameters are known. These models are mostly presented as empirical relationships between the constituent parameters. Models that are for estimation are also applied for calculative and evaluative purposes.

Nwoye (2008) derived a model for evaluating the final pH of the leaching solution during leaching of iron oxide ore in oxalic acid solution. The model evaluates the pH value as the sum of two parts, involving the % concentrations of Fe and Fe<sub>2</sub>O<sub>3</sub> dissolved. The model can be expressed as;

$$\gamma = 0.5 \left[ \frac{K_1}{\%Fe} + \frac{K_2}{\%Fe_2O_3} \right] \quad (1)$$

Where

K<sub>1</sub> and K<sub>2</sub> = Dissolution constants of Fe and Fe<sub>2</sub>O<sub>3</sub> respectively.

γ = Final pH of leaching solution (after time t).

It was also found that the model (Nwoye,2008) could predict the concentration of Fe or Fe<sub>2</sub>O<sub>3</sub>

dissolved in the oxalic acid solution at a particular final solution pH by taking Fe or Fe<sub>2</sub>O<sub>3</sub> as the subject formular. The prevailing process conditions under which the model works include: leaching time of 30mins., constant leaching temperature of 30°C, average ore grain size; 150μm and 0.1M oxalic acid.

Nwoye (2008) has reported that the heat absorbed by oxalic acid solution during leaching of iron oxide ore can be predicted using the model he derived which works under the process condition; initial pH 6.9, average ore grain size; 150μm and leaching temperature; 30°C. The model (Nwoye,2008) can be stated as

$$Q = K_N \left[ \frac{\gamma}{\%Fe_2O_3} \right] \quad (2)$$

Where

Q = Quantity of heat absorbed by oxalic acid solution during the leaching process. (J)

γ = Final pH of the leaching solution (at time t).

%Fe<sub>2</sub>O<sub>3</sub> = Concentration of haematite dissolved in oxalic acid solution during the leaching process.

K<sub>N</sub> = 4.57(Haematite dissolution constant in oxalic acid solution) determined in the experiment (Nwoye,2008).

Nwoye (2008) carried out further work on the model using the same process conditions and observed that on re-arranging the model as;

$$\%Fe_2O_3 = K_N \left[ \frac{\gamma}{Q} \right] \quad (3)$$

the concentrations of haematite predicted deviated very insignificantly from the corresponding experimental values. In this case, the value of  $Q$  was calculated by considering the specific heat capacity of oxalic acid. Values of heat absorbed by the oxalic acid solution during the leaching of iron oxide ore as predicted by the model (Nwoye,2008) agree with the experimental values that the leaching process is endothermic. This is because all the predicted values of the heat absorbed by the oxalic acid solution were positive. The model shows that the quantity of heat absorbed by oxalic acid solution during the leaching process is directly proportional to the final pH of the solution and inversely proportional to the concentration of haematite dissolved.

Model has been derived (Nwoye et al. 2009) for calculating the concentration of leached iron during leaching of iron oxide ore in sulphuric acid solution. The model is expressed as;

$$\%Fe = e^{-2.0421(\ln T)} \quad (4)$$

The model was found to predict %Fe (leached) very close to the values obtained from the experiment, being dependent on the values of the final leaching solution temperature measured during the leaching process. It was observed that the validity of the model is rooted in the expression  $\ln(\%Fe) = N(\ln T)$  where both sides of the expression are correspondingly approximately equal. The positive or negative deviation of each of the model-predicted values of %Fe (leached) from those of the experimental values was found to be less than 37%.

Nwoye et al. (2009) derived a model for predicting the final solution pH at determined initial pH and leaching time during leaching of iron oxide ore in hydrogen peroxide solution. It was observed that the validity of the model is rooted in the mathematical expression;  $(\ln t)^{1/2} = N(\beta^C/\alpha^C)$  where both sides of the relationship are approximately equal to 2. The model is expressed as;

$$\beta = \text{Antilog}[0.2439 \text{Log}(\alpha^{4.1}(\ln t)^{1/2}/3.6)] \quad (5)$$

The model shows that the initial solution pH is dependent on the values of the final solution pH and leaching time. The respective positive or negative deviation of the model-predicted final pH from its corresponding experimental value was found to be less than 8%, which is quite within the acceptable

deviation limit of experimental results depicting the validity of the model.

Model for predictive analysis of the concentration of dissolved iron during leaching of iron oxide ore in sulphuric acid solution was derived by Nwoye et al. (2009). The model expressed as;

$$\%Fe = 0.987(\mu/T) \quad (6)$$

was found to predict %Fe dissolved with high degree of precision being dependent on the values of the leaching temperature and weight of iron oxide ore added. It was observed that the validity of the model is rooted in the expression  $\%Fe = N(\mu/T)$  where both sides of the relationship are correspondingly approximately equal. The positive or negative deviation of each of the model-predicted values of %Fe (dissolved) from those of the experimental values was found to be less than 19% which is quite within the acceptable range of deviation limit for experimental results, hence depicting the usefulness of the model as a tool for predictive analysis of the dissolved iron during the process.

Model for calculating the solution pH during hydrogen peroxide leaching of iron oxide ore has also been derived by Nwoye et al (2009). It was observed that the validity of the model is rooted in the expression  $\ln \gamma = K_C[(\%Fe_2O_3/\%Fe)^N]$  where both sides of the equation are correspondingly approximately equal to 2. The model expressed as;

$$\gamma = \exp \left[ K_C [(\%Fe_2O_3/\%Fe)^N] \right] \quad (7)$$

The final solution pH was found to depend on the values of the % concentrations of dissolved iron and haematite from experiment. The respective deviation of the model-predicted pH values from the corresponding experimental values was found to be less than 20% which is quite within the acceptable range of deviation limit of experimental results.

Model for evaluation of the concentration of dissolved phosphorus (relative to the final pH of the leaching solution) during leaching of iron oxide ore in oxalic acid solution has been derived by Nwoye (2009). The model is expressed as;

$$P = e^{(12.25/\alpha)} \quad (8)$$

Where

$P$  = Concentration of phosphorus removed during the leaching process (mg/Kg)

$N = 12.25$ ; (pH coefficient for phosphorus dissolution in oxalic acid solution) determined in the experiment (Nwoye,2003).

$\alpha$  = Final pH of the leaching solution at the time  $t$  when the concentration of dissolved phosphorus is evaluated.

It was observed that the validity of the model is rooted in the relationship  $\ln P = N/\alpha$  where both sides of the expression are approximately equal to 4. The model depends on the value of the final pH of the leaching solution which varies with leaching time. In all, the positive or negative deviation of the model-predicted phosphorus concentration from its corresponding value obtained from the experiment was found to be less than 22%, which is quite within the acceptable deviation limit of experimental results hence establishing the validity and precision of the model.

Nwoye et al. (2008) derived a model for evaluation of the concentration of dissolved iron (relative to the final solution pH and temperature) during leaching of iron oxide ore in sulphuric acid solution. It was observed that the validity of the model was rooted in expression  $(\%Fe/N)^{1/3} = \alpha/T$  where both sides of the expression are approximately equal to 0.2. The model is expressed as;

$$\%Fe = 0.35(\alpha/T)^3 \quad (9)$$

Where

T= Solution temperature at the time t when the concentration of dissolved iron is evaluated.( $^{\circ}C$ )

N = 0.35(pH coefficient for sulphuric acid solution during leaching of iron oxide ore) determined in the experiment (Nwoye,2007).

$\alpha$  = Final pH of the leaching solution at the time t when the concentration of dissolved iron is evaluated.

The model is dependent on the values of the final pH and temperature of the leaching solution which varied with leaching time.

Application of models for estimating, predicting, evaluating and computational analysis of output process parameters during drying of wet clay have also been reported.

Nwoye (2008) derived a model for calculating the volume shrinkage resulting from the initial air-drying of wet clay. The model;

$$\theta = \gamma^3 - 3\gamma^2 + 3\gamma \quad (10)$$

calculates the volume shrinkage when the value of dried shrinkage  $\gamma$ , experienced during air-drying of wet clays is known. The model was found to be third-order polynomial in nature. Olokoro clay was found to have the highest shrinkage during the air drying condition, followed by Ukpok clay while Otamiri clay has the lowest shrinkage. Volume shrinkage was discovered to increase with increase in dried shrinkage until maximum volume shrinkage was reached, hence a direct relationship.

Nwoye et al. (2008) derived a model for the evaluation of overall volume shrinkage in molded clay products (from initial air-drying stage to

completion of firing at a temperature of  $1200^{\circ}C$ ). It was observed that the overall volume shrinkage values predicted by the model were in agreement with those calculated using conventional equations. The model;

$$S_T = \alpha^3 + \gamma^3 - 3(\alpha^2 + \gamma^2) + 3(\alpha + \gamma) \quad (11)$$

depends on direct values of the dried  $\gamma$  and fired shrinkage  $\alpha$  for its precision. Overall volume shrinkage was found to increase with increase in dried and fired shrinkages until overall volume shrinkage reaches maximum.

Model for calculating the quantity of water lost by evaporation during oven drying of clay at  $90^{\circ}C$  has been derived (Nwoye,2009). The model;

$$\gamma = \exp[(\ln t)^{1.0638} - 2.9206] \quad (12)$$

indicated that the quantity of evaporated water,  $\gamma$  during the drying process is dependent on the drying time t, the evaporating surface being constant. The validity of the model was found to be rooted in the expression  $(\text{Log}\beta + \ln\gamma)^N = \ln t$ .

Model for predictive analysis of the quantity of water evaporated during the primary-stage processing of a bioceramic material sourced from kaolin has been derived by Nwoye et al. (2009). The model;

$$\alpha = e^{(\ln t/2.1992)} \quad (13)$$

shows that the quantity of water  $\alpha$ , evaporated at  $110^{\circ}C$ , during the drying process is also dependent on the drying time t, where the evaporating surface is constant. It was found that the validity of the model is rooted on the expression  $(\ln t/\ln\alpha)^N = \text{Log}\beta$  where both sides of the expression are correspondingly approximately equal to 3. The respective deviation of the model-predicted quantity of evaporated water from the corresponding experimental value was found to be less than 22% which is quite within the acceptable deviation range of experimental results.

Model for quantifying the extent and magnitude of water evaporated during time dependent drying of clay has been derived (Nwoye et al. 2009). The model;

$$\gamma = \exp((\ln t/2.9206)^{1.4}) \quad (14)$$

indicates that the quantity of evaporated water  $\gamma$  during the drying process (at  $90^{\circ}C$ ) is dependent on the drying time, t the evaporating surface being constant. It was found that the validity of the model is rooted in the expression  $\ln\gamma = (\ln t/\text{Log}\beta)^N$  where both sides of the expression are correspondingly almost equal.

Model application has also been extended to the areas of welding and fabrication to predict the hardness a material cooled in a particular medium

relative to the singular or combined hardness of different materials welded and cooled under the same conditions.

Nwoye et al. (2009) derived a model for predictive analysis of hardness of the heat affected zone in aluminum weldment cooled in groundnut oil. The general model;

$$\beta = 0.5997\sqrt{(\gamma\alpha)} \quad (15)$$

is dependent on the hardness of the heat affected zone (HAZ) in mild steel and cast iron weldments cooled in same media. Furthermore, re-arrangement of these models could be done to evaluate the HAZ hardness of mild steel or cast iron respectively as in the case of aluminum. The respective deviations of the model-predicted HAZ hardness values  $\beta$ ,  $\gamma$  and  $\alpha$  from the corresponding experimental values was less 0.02% indicating the reliability and validity of the model.

Quadratic and linear models have also been derived (Nwoye,2009) for predicting the HAZ hardness of air cooled cast iron weldment in relation to the combined and respective values of HAZ hardness of aluminum and mild steel welded and cooled under the same conditions. It was discovered that the general model;

$$\theta = \left( \frac{2.9774\beta - \gamma}{2} \right) + \sqrt{\left( \left( \frac{\gamma - 2.9774\beta}{2} \right)^2 - \gamma\beta \right)} \quad (16)$$

predicts the HAZ hardness of cast iron weldment cooled in air as a function of the HAZ hardness of both aluminum and mild steel welded and cooled under the same conditions. The linear models;  $\theta = 2.2391\gamma$  and  $\theta = 1.7495\beta$  on the other hand predict the HAZ hardness of cast iron weldment cooled in air as a function of the HAZ hardness of aluminum or mild steel welded and cooled under the same conditions. Re-arrangement of the general model also resulted to the evaluation of the corresponding HAZ hardness in aluminum and mild steel weldments

$$\gamma = \left( \frac{2.9774\theta\beta - \theta^2}{\beta + \theta} \right) \quad (17)$$

$$\beta = \left( \frac{\gamma\theta + \theta^2}{2.9774\theta - \gamma} \right) \quad (18)$$

It was found that the validity of the model is rooted on the fractional expression;  $\gamma/2.9774\theta + \gamma/2.9774\beta + \theta/2.9774\beta = 1$  since the actual computational analysis of the expression was also equal to 1, apart from the fact that the expression comprised the three metallic materials. The respective deviations of the model-predicted HAZ hardness values  $\theta$ ,  $\gamma$ , and  $\beta$  from the corresponding experimental values  $\theta_{exp}$ ,  $\gamma_{exp}$ , and  $\beta_{exp}$  was less than 0.003% indicating the validity and reliability of the model.

The aim of this work is to derive models for comparative analysis, assessment and adoption of preferred experimental techniques. Experimental data from past report (Nwoye,2000) will be used for validation of the models.

**2. Methodology and Model Formulation**

The values from Techniques Z, N and K as listed in Tables 3 and 5 were obtained by subtracting for each row in Tables 1 and 2, the lower value from the one directly on its top. The subtraction process is carried out down each column as indicated by the arrows. Assuming Table 1 shows increase in the associated parameter 'electric current' down the column for all Techniques used, it follows that based on the mode of subtraction; the values as presented in Table 3 must all be negative showing increment down the columns.

Table 1: Comparison of data obtained by application of Techniques Z, N and K

Tech. Z	Tech. N	Tech. K	RIS
c <sub>1</sub>	r <sub>1</sub>	e <sub>1</sub>	x <sub>1</sub>
c <sub>2</sub>	r <sub>2</sub>	e <sub>2</sub>	x <sub>2</sub>
c <sub>3</sub>	r <sub>3</sub>	e <sub>3</sub>	x <sub>3</sub>
c <sub>4</sub>	r <sub>4</sub>	e <sub>4</sub>	x <sub>4</sub>
c <sub>5</sub>	r <sub>5</sub>	e <sub>5</sub>	x <sub>5</sub>
c <sub>6</sub>	r <sub>6</sub>	e <sub>6</sub>	x <sub>6</sub>
c <sub>7</sub>	r <sub>7</sub>	e <sub>7</sub>	x <sub>7</sub>
c <sub>8</sub>	r <sub>8</sub>	e <sub>8</sub>	x <sub>8</sub>





Table 2: Comparison of data obtained by application of Techniques Z, N and K

Tech. Z	Tech. N	Tech. K	RIS
v <sub>11</sub>	r <sub>11</sub>	e <sub>11</sub>	x <sub>1</sub>
v <sub>22</sub>	r <sub>22</sub>	e <sub>22</sub>	x <sub>2</sub>
v <sub>33</sub>	r <sub>33</sub>	e <sub>33</sub>	x <sub>3</sub>
v <sub>44</sub>	r <sub>44</sub>	e <sub>44</sub>	x <sub>4</sub>
v <sub>55</sub>	r <sub>55</sub>	e <sub>55</sub>	x <sub>5</sub>
v <sub>66</sub>	r <sub>66</sub>	e <sub>66</sub>	x <sub>6</sub>
v <sub>77</sub>	r <sub>77</sub>	e <sub>77</sub>	x <sub>7</sub>
v <sub>88</sub>	r <sub>88</sub>	e <sub>88</sub>	x <sub>8</sub>



Similarly, assuming Table 2 shows decrement in the associated parameter 'electrical resistance' down the column for all Techniques used, it invariably follows that based on the mode of subtraction; the values as presented in Table 5 must all be positive, showing decrement down the column as indicated by the arrow. Following the subtraction operation, total change in the parameter

for each column of Tables 1 and 2 were evaluated as  $\sum\Phi$  for summation of increments and  $\sum\theta$  for summation of decrements. Average change (increment or decrement) in the parameter down each columns of Tables 1 and 2 were also evaluated as  $\Phi_m$  for average increments and  $\theta_m$  for average decrements.

The Row Identification Symbol (RIS) designated for the experimental data in Tables 1 and 2 are  $x_1, x_2, x_3, x_4, x_5, x_6, x_7$  and  $x_8$ .

Based on the foregoing,

**For increment**

$$\sum\Phi = \sum \left[ (x_1 - x_2) + (x_2 - x_3) + (x_3 - x_4) \dots \right] \quad (19)$$

Equation (19) can also be presented as

$$\sum\Phi = \sum \left[ (x_1 - x_n) + (x_n - x_{n+1}) + (x_{n+1} - x_{n+2}) \right] \quad (20)$$

Where  $n = 2$

Since we have 7 sets of values in each column of Tables 3 and 4 which contains evaluated data,

$$\Phi_m = \frac{\sum \left[ (x_1 - x_n) + (x_n - x_{n+1}) + (x_{n+1} - x_{n+2}) \dots \right]}{N} \quad (21)$$

Where  $n = 2$  and  $N = 7$

Mathematically in evaluating increment, the smaller value is subtracted from the bigger value. However, in this analysis, the values below which are bigger were subtracted from the smaller (on top of it). In consideration of this factor,  $\sum\Phi$  which is negative is multiplied by negative sign to get a real value. Based on this correction, equation (19) becomes;

$$\sum\Phi = -\sum \left[ (x_1 - x_n) + (x_n - x_{n+1}) + (x_{n+1} - x_{n+2}) \right] \quad (22)$$

And equation (20) becomes

$$\Phi_m = -\frac{\sum \left[ (x_1 - x_n) + (x_n - x_{n+1}) + (x_{n+1} - x_{n+2}) \right]}{N} \quad (23)$$

**For decrement**

$$\sum\theta = \sum \left[ (x_1 - x_n) + (x_n - x_{n+1}) + (x_{n+1} - x_{n+2}) \right] \quad (24)$$

Where  $n = 2$

And

$$\theta_m = \frac{\sum \left[ (x_1 - x_n) + (x_n - x_{n+1}) + (x_{n+1} - x_{n+2}) \right]}{N} \quad (25)$$

Where  $n = 2$  and  $N = 7$

Based on the foregoing, equations (22), (23), (24) and (25) are the derived models for analyzing and assessing the experimental data in Tables 1 and 2. Since the analysis carried out using these models involves evaluating the difference (DI) followed by summation operation (SUM) and determining the average value (A), the model for convenience is referred to as DISUMA model.

Table 3: DISUMA analysis showing increments in electric current down the column of Table 1

Tech. A	Tech. B	Tech. C
-d <sub>1</sub>	-h <sub>1</sub>	-p <sub>1</sub>
-d <sub>2</sub>	-h <sub>2</sub>	-p <sub>2</sub>
-d <sub>3</sub>	-h <sub>3</sub>	-p <sub>3</sub>
-d <sub>4</sub>	-h <sub>4</sub>	-p <sub>4</sub>
-d <sub>5</sub>	-h <sub>5</sub>	-p <sub>5</sub>
-d <sub>6</sub>	-h <sub>6</sub>	-p <sub>6</sub>
-d <sub>7</sub>	-h <sub>7</sub>	-p <sub>7</sub>

$$\sum\Phi = -GR; \quad \sum\Phi = -QD; \quad \sum\Phi = -NY$$

$$\Phi_m = -WR; \quad \Phi_m = -MD; \quad \Phi_m = -FY$$

Table 4: DISUMA analysis of Table 1 showing corrected values of increments in electric current obtained in Table 5

Tech. A	Tech. B	Tech. C
d <sub>1</sub>	h <sub>1</sub>	p <sub>1</sub>
d <sub>2</sub>	h <sub>2</sub>	p <sub>2</sub>
d <sub>3</sub>	h <sub>3</sub>	p <sub>3</sub>
d <sub>4</sub>	h <sub>4</sub>	p <sub>4</sub>
d <sub>5</sub>	h <sub>5</sub>	p <sub>5</sub>
d <sub>6</sub>	h <sub>6</sub>	p <sub>6</sub>
d <sub>7</sub>	h <sub>7</sub>	p <sub>7</sub>

$$\sum\Phi = GR; \quad \sum\Phi = QD; \quad \sum\Phi = NY$$

$$\Phi_m = WR; \quad \Phi_m = MD; \quad \Phi_m = FY$$

Table 5: DISUMA analysis showing decrements in electrical resistance down the column of

Tech. A	Tech. B	Tech. C
j <sub>1</sub>	s <sub>1</sub>	u <sub>1</sub>
j <sub>2</sub>	s <sub>2</sub>	u <sub>2</sub>
j <sub>3</sub>	s <sub>3</sub>	u <sub>3</sub>
j <sub>4</sub>	s <sub>4</sub>	u <sub>4</sub>
j <sub>5</sub>	s <sub>5</sub>	u <sub>5</sub>
j <sub>6</sub>	s <sub>6</sub>	u <sub>6</sub>
j <sub>7</sub>	s <sub>7</sub>	u <sub>7</sub>

$$\sum\theta = DR; \quad \sum\theta = EP; \quad \sum\theta = GY$$

$$\theta_m = HR; \quad \theta_m = MP; \quad \theta_m = TY$$



**3. Model validation**

The formulated models were validated by using experimental data from past report (Nwoye,2000). This was done by substituting the values from the experiment (Nwoye,2000) as presented in Tables 6 and 7 into the models; equations (22), (23), (24) and (25). The result of this substitution regarding the ideal and preferred technique was then compared with the preferred technique as reported in the experiment (Nwoye,2000).

Table 6: Effect of copper addition on electric current flow through the Pb-Sb-Cu alloy (Nwoye,2000)

%Cu	Tech. A	Tech. B	Tech. C
0.990	0.215	0.215	0.215
1.961	0.235	0.232	0.238
2.912	0.238	0.238	0.238
3.475	0.240	0.238	0.242
4.762	0.244	0.246	0.242
5.123	0.255	0.253	0.257
6.542	0.264	0.264	0.264
8.257	0.290	0.288	0.286

Table 7: Effect of copper addition on electrical resistance of the Pb-Sb-Cu alloy (Nwoye,2000)

%Cu	Tech. A	Tech. B	Tech. C
0.990	13.4884	13.4884	13.4884
1.961	12.3404	12.5000	12.1850
2.912	12.1849	12.1849	12.1849
3.475	12.0833	12.1849	11.9835
4.762	11.8852	11.7886	11.9835
5.123	11.4625	11.2840	11.3730
6.542	10.9848	10.9848	10.9848
8.257	10.0000	10.0694	10.1399

**4. Results and discussion**

DISUMA analysis of Tables 6 and 7 are shown in Tables 8-12. Tables 10 and 11 are the DISUMA analysis of Table 6 which shows the result of current flowing through the alloys produced using Technique A, B and C. The parameters  $\sum\Phi$  and  $\Phi_m$  when corrected in equations (22) and (23) gives Technique A the greatest values followed by that of Technique B and Technique C. This implies that the totality of the current flow through Pb-Sb-Cu alloys cast using Technique A is the highest followed by that of Technique B and then Technique C. This invariably shows that alloys made by simultaneous addition of Cu powder and pouring of the molten Pb-Sb into the mould (Technique A) permits better current flow. Table 12 is the DISUMA analysis of Table 7. This analysis also shows from the values of  $\sum\theta$  and  $\theta_m$  that total drop in electrical resistance is greatest in

Technique A followed by Technique B and then C. This also implies that more current would be permitted to flow in Technique A compared to Techniques B and C. This agrees with the result of the experiment earlier reported (Nwoye,2000).

Table 8: Modified form of Table 1 showing symbols assigned to each row of values

%(Cu)	Tech. A	Tech. B	Tech. C	RIS
0.990	0.215	0.215	0.215	$x_1$
1.961	0.235	0.232	0.238	$x_2$
2.912	0.238	0.238	0.238	$x_3$
3.475	0.240	0.238	0.242	$x_4$
4.762	0.244	0.246	0.242	$x_5$
5.123	0.255	0.253	0.257	$x_6$
6.542	0.264	0.264	0.264	$x_7$
8.257	0.290	0.288	0.286	$x_8$

Table 9: Modified form of Table 2 showing symbols assigned to each row of values

%(Cu)	Tech. A	Tech. B	Tech. C	RIS
0.990	13.4884	13.4884	13.4884	$x_1$
1.961	12.3404	12.5000	12.1850	$x_2$
2.912	12.1849	12.1849	12.1849	$x_3$
3.475	12.0833	12.1849	11.9835	$x_4$
4.762	11.8852	11.7886	11.9835	$x_5$
5.123	11.4625	11.2840	11.3730	$x_6$
6.542	10.9848	10.9848	10.9848	$x_7$
8.257	10.0000	10.0694	10.1399	$x_8$

Table 10: DISUMA analysis showing increments in electric current down the column of Table 1

Tech. A	Tech. B	Tech. C
-0.020	-0.017	-0.023
-0.003	-0.006	-0.000
-0.002	-0.000	-0.004
-0.004	-0.008	-0.000
-0.011	-0.007	-0.015
-0.009	-0.011	-0.007
-0.026	-0.024	-0.022

$\sum\Phi = -0.075$ ;  $\sum\Phi = -0.073$ ;  $\sum\Phi = -0.071$   
 $\Phi_m = -0.0107$ ;  $\Phi_m = -0.0104$ ;  $\Phi_m = -0.0101$

Table 11: DISUMA analysis of Table 1 showing corrected values of increments in electric current obtained in Table 5

Tech. A	Tech. B	Tech. C
1.1480	0.9884	1.3034
0.1555	0.3151	0.0001
0.1016	0.0000	0.2014
0.1981	0.3963	0.0000
0.4227	0.5046	0.6105
0.4777	0.2992	0.3882
0.9848	0.9154	0.8449

$$\sum\Phi = 0.075; \sum\Phi = 0.073; \sum\Phi = 0.071$$

$$\Phi_m = 0.0107; \Phi_m = 0.0104; \Phi_m = 0.0101$$

Table 12: DISUMA analysis showing decrements in electrical resistance down the column of Table 2

Tech. A	Tech. B	Tech. C
0.020	0.017	0.023
0.003	0.006	0.000
0.002	0.000	0.004
0.004	0.008	0.000
0.011	0.007	0.015
0.009	0.011	0.007
0.026	0.024	0.022

$$\sum\theta = 3.4884; \sum\theta = 3.4190; \sum\theta = 3.3485$$

$$\theta_m = 0.4983; \theta_m = \mathbf{0.4884}; \theta_m = 0.4784$$

### Conclusion

Following comparative analysis of the results associated with Pb-Sb-Cu alloys cast using Techniques A, B and C, the model adopted (in agreement with previous studies (Nwoye,2000) Technique A as the ideal and preferred casting technique for production of Pb-Sb-Cu alloys designated for the manufacturing of battery head terminals and plates. This is because greater amount of electric current were permitted to flow through alloys cast using Technique A compared to Techniques B and C.

### Correspondence to:

Chukwuka Ikechukwu Nwoye  
 Department of Materials and Metallurgical  
 Engineering, Federal University of Technology,  
 P.M.B 1526 Owerri. Imo State, Nigeria.  
 Cellular phone: 0803 800 6092  
 Email: [chikeyn@yahoo.com](mailto:chikeyn@yahoo.com)

### References

1. Iwu DH. Statistical Analysis of Processes, 2<sup>nd</sup> edition, Oak Press, Enugu 1996: pp29.
2. Nwoye CI. Model for Quantitative Analysis of Dissolved Iron in Oxalic Acid

Solution during Leaching of Iron Oxide Ore, Inter. Res. J. Eng. Sc. Tech. 2008: 5(1):37-41.

3. Nwoye CI. Model for Computational Analysis of Dissolved Haematite and Heat Absorbed by Oxalic Acid Solution during Leaching of Iron Oxide Ore, J. Eng.& App. Sc. 2008: 4:22-25.
4. Nwoye CI, Obasi GC, Mark U, Inyama S, Nwakwuo CC. Model for Calculating the Concentration of Leached Iron Relative to the Final Solution Temperature during Sulphuric Acid Leaching of Iron Oxide Ore New York Sc. Journal 2009: 2(3):49-54.
5. Nwoye CI, Agu PC, Onukwuli OD, Borode JO, Mbah CN. Model for Predicting the Initial Solution pH at Assumed Final pH and Leaching Time during Leaching of Iron Oxide Ore in Hydrogen Peroxide Solution. New York Sc. Journal 2009: 2(3):43-48
6. Nwoye CI, Ofoegbu SU, Obi MC, Nwakwuo C C. Model for Predictive Analysis of the Concentration of Dissolved Iron Relative to the Weight Input of Iron Oxide Ore and Leaching Temperature during Sulphuric Acid Leaching. Nat. & Sc. J. 2009:7(3):41-47.
7. Nwoye CI, Ejimofor RA, Nlebedim C, Nwoye UC, Obi MC, Obasi GC, Agu PC. Model for Calculating the Solution pH during Hydrogen Peroxide Leaching of Iron Oxide Ore Nat & Sc 2009:7(3):48-54.
8. Nwoye CI. Model for Evaluation of the Concentration of Dissolved Phosphorus during Leaching of Iron Oxide Ore in Oxalic Acid Solution. JMMCE 2009: 8(3):181-188.
9. Nwoye CI. SynchroWell Research Work Report, DFM Unit, No 2031196, 2003:26-60.
10. Nwoye CI, Amara GN, and Onyemaobi OO. Model for Evaluation of the Concentration of Dissolved Iron during Leaching of Iron Oxide ore in Sulphuric Acid Solution. Int. J. Nat. Appl. Sc. 2008:(2):209-211.
11. Nwoye CI. SynchroWell Research Work Report, DFM Unit, No. 2051198, 2007:76-83.
12. Nwoye CI. Mathematical Model for Computational Analysis of Volume Shrinkage Resulting from Initial Air-Drying of Wet Clay Products. International Research Journal of Engineering Science and Technology 2008;5(1):82-85.
13. Nwoye CI, Iheanacho IO and Onyemaobi OO. Model for the Evaluation of Overall Volume Shrinkage in Molded Clay

- Products from Initial Air-Drying Stage to Completion of Firing. *International Journal of Natural & Applied Science* 2008: 4(2), 234-238.
14. Nwoye CI. (2009). Model for Calculating the Quantity of Water Lost by Evaporation during Oven Drying of Clay. *Researcher Journal* 2009: 1(3), 8-13.
  15. Nwoye CI, Okeke K, Obi M, Nwanyanwu U, and Ofoegbu S. Model for Predictive Analysis of the Quantity of Water Evaporated during the Primary-Stage Processing of Bioceramic Material Sourced from Kaolin. *Journal of Nature and Science* 2009: 7(4), 79-84.
  16. Nwoye CI, Nwakwuo CC, Obi MC, Obasi G C, and Onyemaobi OO. Model for Quantifying the Extent and Magnitude of Water Evaporated during Time Dependent Drying of Clay. *New York Journal of Science* 2009: 2(3), 55-58.
  17. Nwoye CI, Odumodu U, Nwoye CC, Obasi G C, and Onyemaobi OO. Model for Predictive Analysis of Hardness of the Heat Affected Zone in Aluminum Weldment Cooled in Groundnut Oil Relative to HAZ Hardness of Mild Steel and Cast Iron Weldments Cooled in Same Media. *New York Sc. J.* 2009:2(6):93-98.
  18. Nwoye CI. Quadratic and Linear Models for Predicting the Hardness of Heat Affected Zone in Air Cooled Cast Iron Weldment in Relation to the HAZ Hardness of Aluminum and Mild Steel Weldments Cooled in Same Media. *Res. J.* 2009: 1(4):1-6.
  19. Nwoye CI. Effect of Copper Powder Dispersion on the Electrical Conductivity of Lead-Antimony Alloy, M. Eng. Thesis, Nnamdi Azikiwe University, Awka, Nigeria 2000.

6/19/2009